HARD X-RAY SELF-SEEDING SETUP AND RESULTS AT SACLA

T. Inagaki#, T. Tanaka, N. Adumi, T. Hara, R. Kinjo, H. Maesaka, Y. Otake, K. Togawa, M. Yabashi, H. Tanaka, T. Ishikawa, RIKEN SPring-8 Center, Sayo, Hyogo, Japan
Y. Inubushi, T. Kameshima, H. Kimura, A. Miura, H. Ohashi, T. Ohata, K. Tono, H. Yamazaki, S. Goto, Japan Synchrotron Radiation Research Insititute, Sayo, Hyogo, Japan
T. Hasegawa, S. Tanaka, SPring-8 service Co. Ltd., Sayo, Hyogo, Japan

Abstract

A self-seeded XFEL system using a Bragg transmission scheme has been implemented at the compact XFEL facility SACLA, in order to generate a single-mode XFEL. The setup is composed of a small magnetic chicane that can delay the electron beam by up to 50 fs, and a diamond single crystal with the thickness of 180 μm. In the beam commissioning, intensity enhancement at 10 keV X-rays due to the self-seeding was observed with a single-shot spectrometer. A spectral bandwidth of the seeded FEL was reduced to 3 eV, being approximately 1/10 of that of SASE. After partial optimizations of the number of undulator segments, a temporal delay of the electron beam, and an rf phase of the pre-buncher cavity, the peak intensity of the seeded FEL signal in the averaged spectrum was 4 times higher than the SASE. Observation probability of the seeded FEL signal in the single-shot spectra was 42%. Although further optimization and improvement are still necessary to keep long-term stability, the initial step was successful to open up the routine operation in a near future.

INTRODUCTION

Self-seeding in the X-ray free electron laser (XFEL) is an important method to improve the temporal coherence of the self-amplified spontaneous emission (SASE) and to obtain high peak brilliance with narrow spectral band width. In order to generate brilliant X-ray laser and supply to user experiments, the self-seeding system has been implemented in the Japanese XFEL facility, SPring-8 Angstrom Compact free electron LAser (SACLA) [1]. The scheme proposed at DESY [2] and firstly demonstrated in LCLS [3] was adopted, which uses a single diamond crystal in a forward Bragg diffraction (FBD) geometry to the initial SASE radiation from the first half of the undulators. It produces monochromatic tail components of transmitted X-ray pulses at a small time delay of several 10 fs. A compact magnetic chicane gives the delay to overlap the electron bunches and the monochromatic tail for seeding in the following undulators.

The hardware components were installed in parallel to the user operation from 2012. In August 2013, a vacuum chamber for housing a diamond single crystal was installed in the middle of the magnetic chicane. The commissioning started in October. After a number of tuning processes, significant spectral narrowing due to the self-seeding was confirmed at 10 keV. In the following sections, the configuration, the tuning process and the experimental results are described.

#inagaki@spring8.or.jp

SETUP

Figure 1 shows the configuration of SACLA and the self-seeding system. The electron beam from the thermionic cathode-type electron gun is sequentially accelerated and compressed at the accelerator section, to obtain high-density electron beam with the peak current of over several kA and the bunch length of several 10 fs. Then, the electron beam is led to the long undulator section composed of 21 segments of the in-vacuum undulators with the small periodic length of λ_u=18 mm and the maximum K-value (the magnetic deflection parameter) of 2.2.

Between the 8th undulator and the 9th undulator, the small magnetic chicane composed of 4 dipole magnets was inserted, in order to detour the electron beam from the diamond crystal and to provide a tunable time delay of maximum 50 fs. In the middle of the chicane, the diamond crystal chamber was installed, in order to generate the FBD of the SASE radiation from the upstream undulators. Figure 2 shows the schematic of the chamber. A diamond single crystal with the thickness of 180 μm is mounted on a holder in the vacuum chamber. The holder is attached on a multi-axis mechanical stage. The crystal is retracted from the beam axis during the usual SASE operation, while it is inserted for the self-seeding. The rotation of the crystal tuned the Bragg angle θ. The diffracted photon is measured by a photo-diode and a CCD detectors, attached on the 2θ-rotational arm. Since the photon energy for our commissioning was 10 keV, the Bragg angle θ was set at about 44 degrees for 400 reflection of the diamond crystal. Under these configurations, monochromatic tail components in the transmitted radiation arise around 10 fs and 24 fs after the initial radiation, according to the theoretical calculation of FBD [3, 4]. The electron beam delaying at the chicane was overlapped to the radiation in the downstream undulators.

Properties of the FEL radiation were measured at the experimental hall. Thin-foil beam monitors in the optics hutch were used as the in-line monitors of the intensity and the center-of-mass position of the radiation [5]. The energy spectrum of the radiation was measured by the single-shot spectrometer [6]. The spectral resolution and the range are selected by changing the diffraction plane of the silicon crystal. The configuration using (220) plane has a wide measuring range of 100 eV, which was used

ISBN 978-3-95450-133-5

Copyright © 2014 CC-BY-3.0 and by the respective authors

for the measurement of the whole radiation spectrum. The configuration using (660) plane has a narrow measuring range of 6 eV, but it has a high energy resolution of about 70 meV, which was used for the precise measurement around the Bragg diffraction.

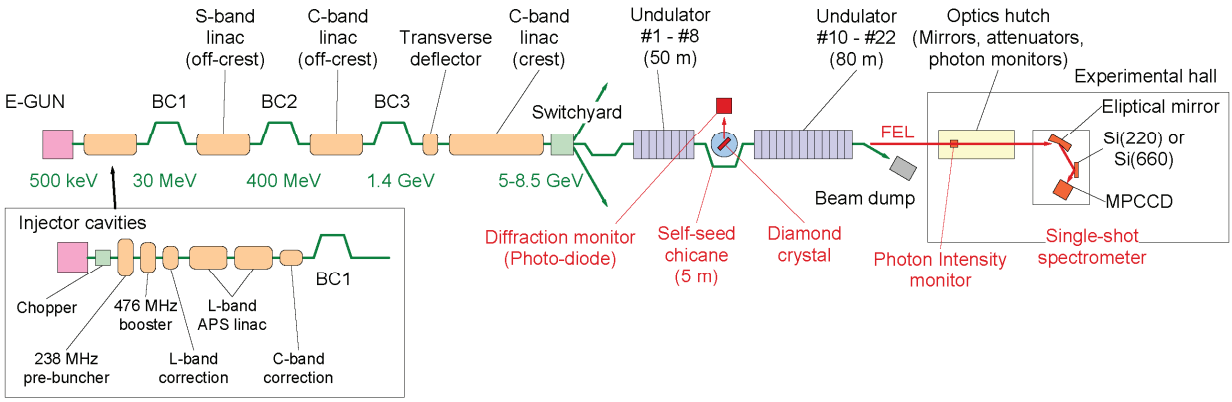

Figure 1: Configuration of the SACLA machine and the self-seeding system. BC1, BC2, and BC3 mean the three bunch compression chicanes.

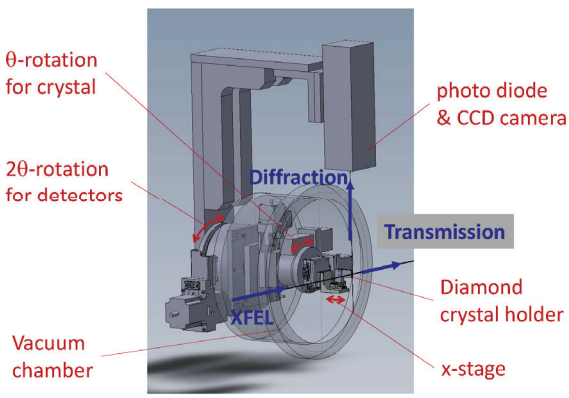

Figure 2: Diamond crystal chamber.

TEST RESULTS

Commissioning of the self-seeding was performed several times during the machine study period of SACLA operation. In November 2013, the first evidence of the seeded radiation was observed in the energy spectrum. After the electron beam stability was improved in May 2014, significant spectrum narrowing due to the self-seeding process was observed. In this section, we report the results of commissioning in June 2014.

The electron beam energy and the photon energy for the commissioning were 7.8 GeV and 10 keV, respectively. The K-value of the undulators was set at about 2.1, with a small taper of -0.002/segment for a compensation of the electron energy loss. The electron bunch charge was about 340 pC. The bunch length was about 30 fs, which was measured using the transverse deflector cavity located after the final bunch compression chicane (BC3). The electron beam quality was confirmed by measuring the SASE pulse energy of about 550 μJ/pulse, using all of 21 undulator segments and without the crystal insertion.

Adjustment of the SASE Photon Energy

Four undulator segments (#5-8) in the upstream of the diamond crystal were used to generate initial SASE radiation of about 30 μJ/shot in average. After the dipole magnets at the chicane were turned on to give a delay of 20 fs to the electron beam, the diamond crystal was inserted to the beam axis. The Bragg angle was set at 44 degrees in diamond 400 diffraction for 10 keV radiation. We optimized the undulator K values, to match the wavelength of the SASE radiation to the Bragg diffraction wavelength. Figure 3 shows the diffracted X-ray intensity as a function of the offset from the initial K values. We selected the offset of -0.002, which corresponds to the center of the SASE spectrum.

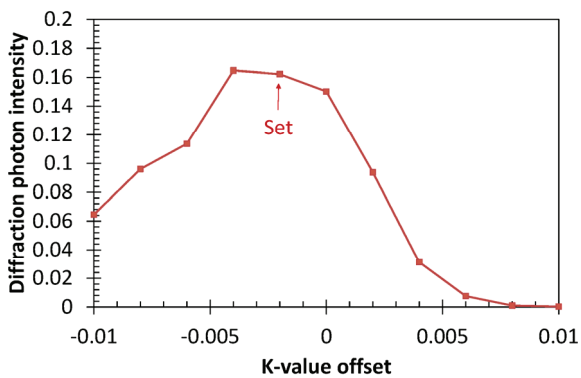

Figure 3: Bragg diffraction intensity measured by the photo-diode as a function of the K-value offset of the upstream undulators.

Spectrum of the Transmitted SASE Radiation

Energy spectrum of the transmitted SASE radiation was measured using the single-shot spectrometer. The diffraction plane of the silicon crystal was set to (660) for high-resolution measurement. Figure 4 shows the typical

Copyright © 2014 CC-BY-3.0 and by the respective authors

ISBN 978-3-95450-133-5

spectrum. We found a clear dip due to the Bragg diffraction of the diamond crystal. The width of the dip was about 0.1 eV (2 pixels of the CCD detector), which was comparable to the measurement resolution. These results proved the diamond crystal has a good quality for raising the FBD and no radiation damage or degradation was observed during the commissioning.

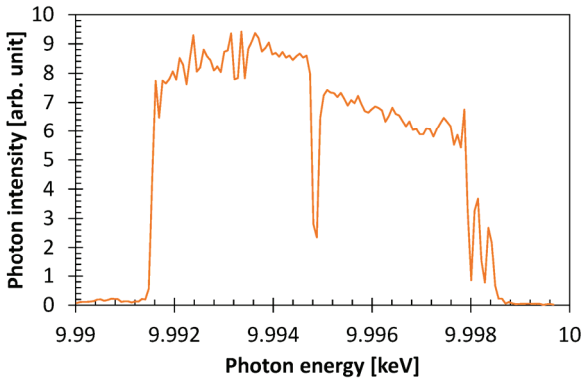

Figure 4: Energy spectrum of the transmitted SASE radiation from the upstream undulators, which was the integration of 100 shots. There was a clear dip at 9.995 keV due to the Bragg diffraction of the diamond crystal.

Observation of the Seeding

After the confirmation of the Bragg diffraction, we closed the gap of the downstream undulators. We measured the photon energy spectrum using the single-shot spectrometer with 220 diffraction plane for wide measuring range of 100 eV. Figure 5 shows the energy spectra with different number of downstream undulator segments. Clear peaks were observed at 9.99 keV photon energy. Increasing the number of undulator segments, the monochromatic X-ray component dominantly increased. With all of 13 undulator segments (blue line in Figure 5), the peak intensity of the monochromatic component was 4 times higher than the SASE background. The spectral bandwidth was 3 eV in FWHM, which was one order narrower than that for SASE. For the confirmation, we detached the diamond crystal from the SASE photon axis. Then the monochromatic component disappeared. We concluded the enhancement of the monochromatic component was surely due to the self-seeding from the FBD of the diamond crystal. Since Figure 4 and Figure 5 were measured with different configuration of the spectrometer, the photon energy difference between the Bragg diffraction in Figure 4 and the seeded FEL peak in Figure 5 was not obvious and they were within the measurement error.

In the following subsections, we describe the optimization of various parameters and the sensitivity study for the accelerator.

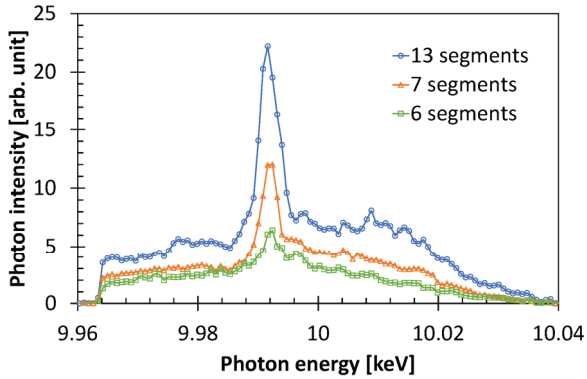

Figure 5: Energy spectra of the X-ray radiation with the seeding configuration. The three lines show the spectra with different number of active undulator segments at the downstream of the chicane. The spectra were the integration of 100 shots.

Number of Undulator Segments

Figure 6 shows the peak intensity of the seeded monochromatic components and the SASE background, as a function of the number of downstream undulator segments. When we increased the number of undulator segments, the seeded FEL signal also increased, while the SASE background was hardly increased. This result means the radiation from the downstream undulator was fairly monochromatic due to the seeding. In the Figure 6, slight decrease of the seeded FEL intensity with 9 undulator segments was not obvious, because the systematic error and the reproducibility were still larger than the discrepancy of the seeded FEL intensity.

Next we changed the number of upstream undulator segments, fixing the 13 downstream undulator segments. Figure 7 shows the seeded FEL intensity and the SASE background, with 3, 4, 5 or 6 undulator segments. With 3 undulator segments, the seeded FEL signal was not observed. We consider the initial SASE radiation was too weak for the seeding. With 6 undulator segments, the seeded FEL intensity was lower than the case with 4 or 5 undulator segments. It was considered that the SASE radiation process increased the energy spread of the electron beam and it suppressed the seeding. Therefore we concluded the optimum number of upstream undulator was 4 or 5 (corresponding SASE pulse energy was from 30 to 100 μJ/pulse). For the following study, we used 4 and 13 undulator segments in the upstream and downstream, respectively.

Copyright © 2014 CC-BY-3.0 and by the respective authors

ISBN 978-3-95450-133-5

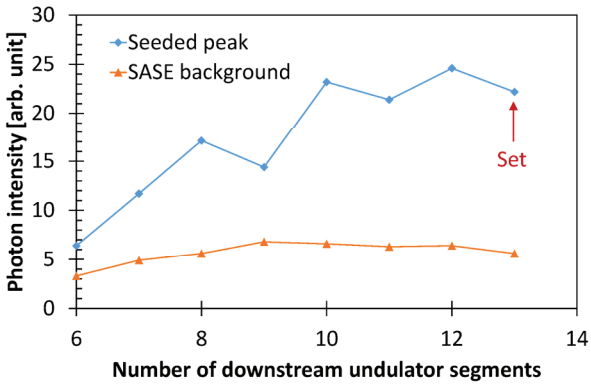

Figure 6: Peak intensity of the seeded monochromatic components and the intensity of the SASE background, as a function of the number of active undulator segments at the downstream of the chicane. For these measurements, 4 upstream undulator segments were used and the delay of the electron beam was set at 20 fs.

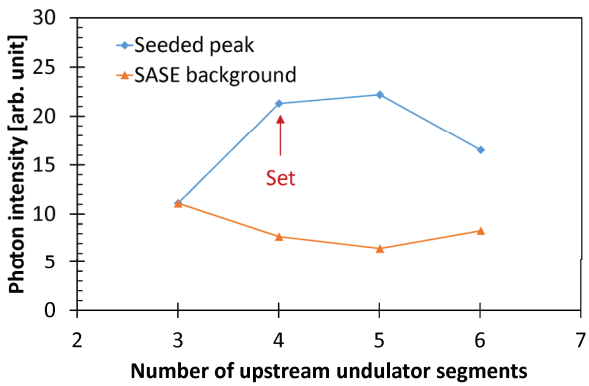

Figure 7: Peak intensity of the seeded monochromatic components and the intensity of the SASE background, depending on the number of active undulator segments at the upstream of the chicane. For these measurements, 13 downstream undulator segments were used and the delay of the electron beam was set at 20 fs.

Delay Time for Electron Beam

Figure 8 shows the seeded FEL signal and the SASE background, as a function of the temporal delay for the electron beam at the chicane. The seeded FEL signal was enhanced with the delay of about 25 fs and 45 fs, which was consistent with the theoretical calculation.

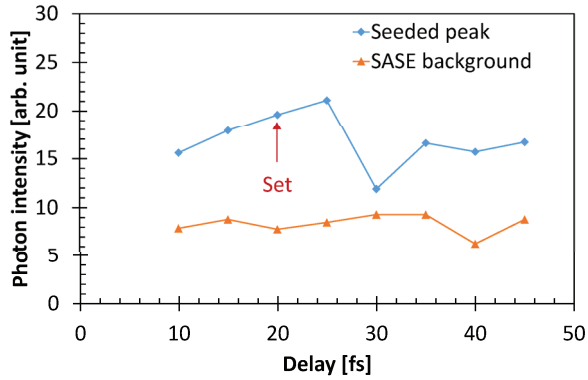

Figure 8: Peak intensity of the seeded monochromatic components and the averaged intensity of the SASE background, depending on the delay time at the chicane.

RF Phase of the Accelerator

In order to optimize the electron beam properties and to check the sensitivity for the rf phase variation, we performed a systematic study changing the rf phase of each accelerator section. Figure 9(d) shows the spectra with different rf phase of the 238 MHz pre-buncher. Only the change of 0.05 degree caused the significant effect for the seeded amplification. Figure (a) (b) and (c) show the variation of the seeded FEL intensity and the overall pulse energy, changing the rf phase of C-band linac between BC2 and BC3 (off-crest acceleration section), L-band APS-type linac and 238 MHz pre-buncher, respectively. They show the seeded FEL intensity was more sensitive to the rf phase variation than the SASE intensity. Table 1 summarizes the rf phase tolerance to maintain the seeded FEL intensity of more than half of the optimum peak intensity. These results indicate that the commissioning for the self-seeding requires higher operational stability and accuracy than the case of usual SASE operation. Actually, the observed spectrum and the peak intensity were sometimes changed during the several hours of the commissioning. These variations might be caused by tiny drifts of the accelerator condition, which were not recognized in usual SASE operation. We should study more to optimize and stabilize the accelerator condition.

Copyright © 2014 CC-BY-3.0 and by the respective authors

ISBN 978-3-95450-133-5

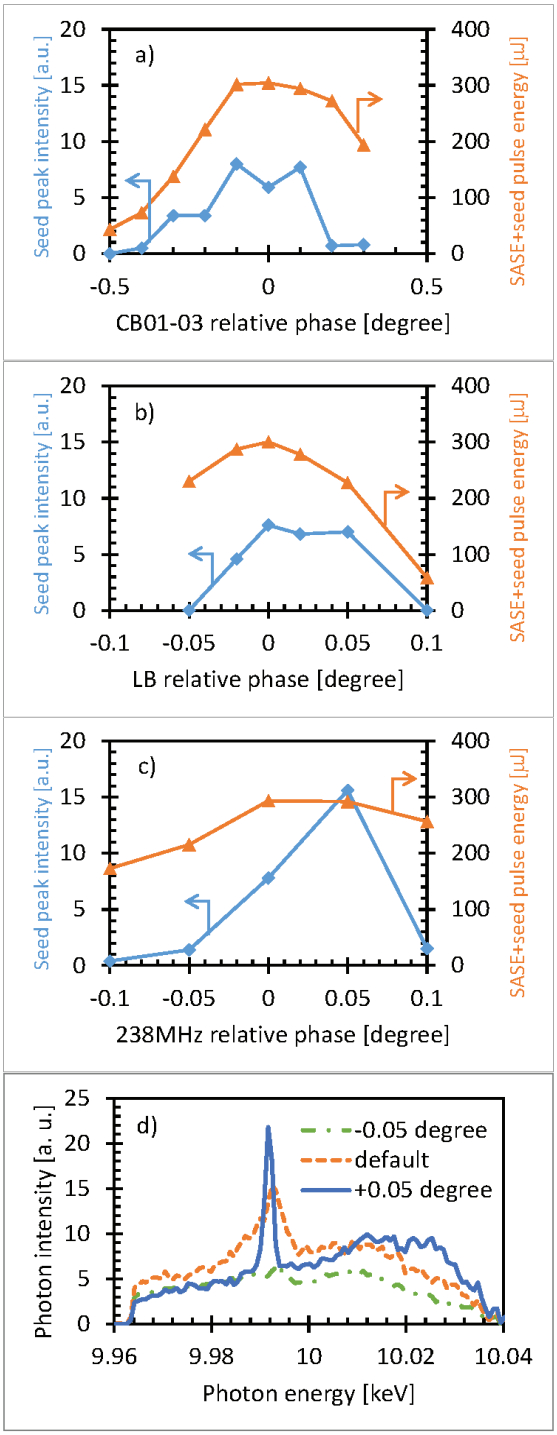

Figure 9: (Plot a, b, and c) Peak intensity of the seeded monochromatic components (Blue line), and the total pulse energy measured by the in-line beam monitor (Orange line), depending on the relative rf phase of the C-band linac before BC3, (a), the L-band APS-type linac (b) and the 238 MHz pre-buncher cavity (c), from the initial operating parameters. Plot d) shows the energy spectra for three rf phases of the 238 MHz pre-buncher cavity. The each spectrum is the integration over 100 shot, measured by the single-shot spectrometer.

Table 1: RF Phase Tolerances and the Corresponding Time Period for Each Accelerator Section. The tolerances in this table are defined as the rf phase difference made 50 % decrease of the seeded FEL intensity

Accelerator section	**Tolerance** (time)
238 MHz pre-buncher	±0.05° (600 fs)
476 MHz booster	±0.1° (600 fs)
L-band APS-type linac	±0.05° (100 fs)
C-band correction cavity	±0.3° (150 fs)
S-band linac	±0.5° (500 fs)
C-band linac (before BC3)	±0.2° (100 fs)

Single-Shot Spectrum

We analysed the single-shot spectrum data with optimum rf parameters, as shown in Figure 9 (d, blue line). Figure 10 shows the distribution of the peak photon energy (wavelength) and the peak intensity of each single-shot spectrum. Since the seeding wavelength is fixed by the Bragg diffraction angle of the diamond crystal, the "seeded" events are distributed around the photon energy of 9.99 keV. We defined the criteria of the "seeded" events, that the photon energy were 9.990±0.005 keV and the peak intensity was more than 20,000 counts (blue dash line in Figure 10). The criteria for the peak intensity was required to distinguish the clear peak from the many small spikes due to the initial SASE background. Then, the probability for observation of the seeded FEL signal which satisfied above criteria was 42%. Averaged peak intensity for the seeded FEL signal was 9 times higher than the averaged intensity of SASE background. Shot-by-shot fluctuation of the peak intensity was 31% in rms. Fluctuation of the photon energy was less than 1 eV, which is comparable to the resolution of the spectrometer. These are promising results for the future practical use of self-seeding in SACLA.

ISBN 978-3-95450-133-5

Copyright © 2014 CC-BY-3.0 and by the respective authors

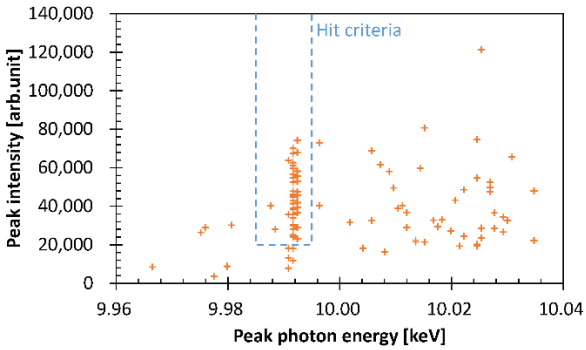

Figure 10: Distribution of the peak photon energy and the peak intensity for each single-shot spectrum, which is the same data set as "+0.05 degree" spectrum in Figure 9 d). Blue dash line box shows the criteria for "seeded" event.

CONCLUSION

In order to generate high-intense, monochromatic X-ray laser, self-seeded XFEL system with forward Bragg diffraction (FBD) of the diamond single crystal has been developed in SACLA. The monochromatic X-ray enhancement and the spectral narrowing due to the seeding were observed at a photon energy of 9.99 keV. The peak intensity of the seeded FEL signal was 4 times higher than the SASE. The probability for observation of the seeded FEL signal in the single-shot spectrum was 42% and the fluctuation of the intensity was 31% in rms. These are promising results for the future practical use of the self-seeding scheme. Since the seeding process is quite sensitive to the rf phase variation, high operational stability and accuracy is necessary for the seeding. Further tuning efforts are continued for stable seeded FEL generation in order to provide seeded XFEL for users.

ACKNOWLEDGMENT

The authors give thanks to Dr. G. Geloni, Dr. J. Hastings, Dr. E. Allaria, Dr. F. Loehl, and Dr. K. Ohmi, for joining our commissioning and having useful discussions. The authors thank all of SACLA staffs for operation of SACLA and construction of self-seeding hardware and software.

REFERENCES

[1] T. Ishikawa, et. al., "A compact X-ray free-electron laser emitting in the sub-angstrom region", Nat. Photonics 6, 540-544 (2012).

[2] G. Geloni, V. Kocharyan, and E. Saldin, "A novel self-seeding scheme for hard X-ray FELs", J. Mod. Opt. 58, 1391-1403 (2011).

[3] J. Amann, et. al., "Demonstration of self-seeding in a hard X-ray free-electron laser", Nat. Photonics 6, 693-698 (2012).

[4] R. Lindberg and Yu Shvydko, "Time dependence of Bragg forward scattering and self-seeding of hard x-ray free electron lasers", Phys. Rev. ST Accel. Beams 15, 050706 (2012).

[5] K. Tono, et. al., "Beamline, experimental stations and photon beam diagnostics for the hard x-ray free electron laser of SACLA", New J. of Phys. 15, 083035 (2013).

[6] Y. Inubushi, et. al., "Determination of the pulse duration of an x-ray free electron laser using highly resolved single-shot spectra", Phys. Rev. Lett. 109, 144801 (2012).

Copyright © 2014 CC-BY-3.0 and by the respective authors

ISBN 978-3-95450-133-5